UNIVERSITAT POLITÈCNICA DE CATALUNYA BARCELONATECH

ESCOLA TÈCNICA SUPERIOR D'ENGINYERIA DE TELECOMUNICACIÓ DE BARCELONA

TREBALL FINAL DEL GRAU EN ENGINYERIA FÍSICA

Simulation and control of a heterogeneous fleet of vehicles

Autor del treball

Alexandre Justo Miro

Barcelona, juny de 2019

Codirigit per

Dr. Josep Maria Olm Miras

Dr. Arnau Dòria Cerezo

UNIVERSITAT POLITÈCNICA DE CATALUNYA BARCELONATECH

ESCOLA TÈCNICA SUPERIOR D'ENGINYERIA DE TELECOMUNICACIÓ DE BARCELONA

Simulation and control of a heterogeneous fleet of vehicles

Alexandre Justo Miro

Barcelona, juny de 2019

Codirigit per

Dr. Josep Maria Olm Miras

Dr. Arnau Dòria Cerezo

Contents

Preface

Motivation

Autonomous driving is an emergent challenge for engineers, being a field where technological development increases exponentially. As a student of the Bachelor's Degree in Engineering Physics, I took the opportunity to undertake this Final Bachelor's Degree Project, as I consider it to be fundamental in my upcoming future, where I wish I can contribute to more development on Autonomous Vehicles.

It was a challenge for me because I had to face new horizons of knowledge, use tools which I had not used never such as Simulink; but motivation and ambition were my fuel. We have been able to explore and break some barriers, which I am very proud of.

Acknowledgements

Firstly, I want to thank all the professors and managers of the Bachelor's Degree in Engineering Physics, since thanks to them I have acquired good knowledge and an extraordinary vision of both the scientific and engineering world.

In particular, to the professors of the Control Theory course, Domingo Biel and Josep M. Olm, who transmitted to me the passion for that topic, which has ended up being nothing else than the basis of this five-month Final Bachelor's Degree Project and, perhaps, the basis of my professional career.

And my special acknowledgements are for the co-directors of my project, Arnau Dòria-Cerezo and Josep M. Olm; who not only provided me with invaluable help, which is indicative of them being superb directors; but also made me feel comfortable and have a good time whenever we were together.

Truthfully, thank you.

Introduction

Traffic is challenging. Everybody wants to drive comfortably and arrive soon to their destination, and nobody wants to be stuck in a traffic jam. But those unfortunate situations are still produced every day. Do autonomous vehicles have something to say to this problem?

In traffic flow dynamics there exists the so-called Stop and Go effect [1]. It is a characteristic which arises from collective human driving behaviour, and it usually appears when the density of vehicles is high enough. Instead of achieving the same speed each one of the individual vehicles, they throttle towards a speed which is above the capability of the road, so that at a point they must brake below it. When they are stopped they throttle again and the process is repeated so on. It is because of it that this project's ultimate objectives are, by means of simulations with controlled autonomous vehicles:

- improve traffic flow; in particular, the average speed of vehicles,
- reduce or eliminate the magnitude of the Stop and Go effect.

Any progress in either case, or in both cases, will make this project useful. However, in order to achieve that, one must first go through many stages.

The first of the goals is to choose the model for human driven vehicles that better imitates the human behavior observed, in particular, in a circular track; by implementing it in MATLAB/Simulink and verifying the results. For the second goal, the circular track is momentarily forgotten. This stage consists of designing a new control-oriented model for heterogeneous traffic flow, consisting of an autonomous vehicle which has a variable-length fleet of human driven vehicles behind. A control algorithm is designed on the basis of that mode. For the third of the goals, when the control algorithm works, a new setup is built in the circular track. It will consist of two intercommunicated autonomous vehicles embedded among a bunch of human driven vehicles. Here is where the traffic flow is checked to either improve or not.

Chapter 1

Longitudinal dynamics of car-following vehicles

From now on, in this work it is going to be assumed that all vehicles travel in a single lane (meaning all vehicles travel in the same lane) and, obviously, there are no overtakes; so a fleet of vehicles will always keep the same order between individuals.

Also the speed of vehicles is going to be restricted to be greater or equal than zero, in order for no reverse gear to be allowed. The acceleration of vehicles, however, does not have any sign restrictions since vehicles are expected to accelerate and decelerate/brake.

Given a pair of vehicles, with subscripts $i-1$ (precedent) and i (chasing), one model generally assumed to work is presented next.

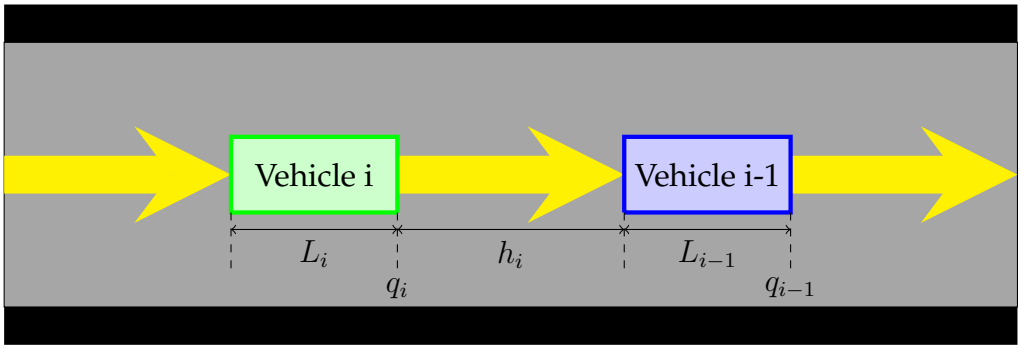

Figure 1.1: A fleet of 2 vehicles with their position taken from their frontal bumpers.

The net bumper-to-bumper distance h, understood as the distance a vehicle has from its frontal bumper to the rear bumper of the vehicle in front, can be defined in two different ways. As in Figure 1, it can be done by taking q from the frontal bumpers:

$$h_i = q_{i-1} - q_i - L_{i-1}; \tag{1.1}$$

or, as in Figure 1, by taking q from the rear bumpers:

$$h_i = q_{i-1} - q_i - L_i. \tag{1.2}$$

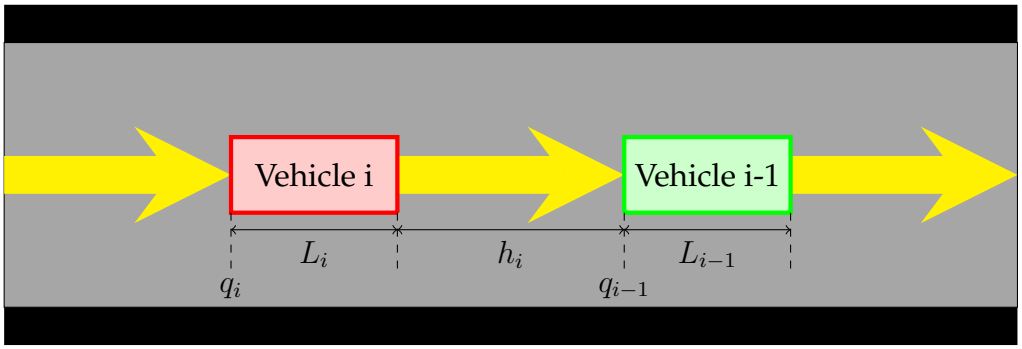

Figure 1.2: A fleet of 2 vehicles with their position taken from their rear bumpers.

The variable h, along with the speed $v = \dot{q}$ and the acceleration a, is a crucial part of the dynamical system presented in (1.3). It considers first order dynamics for v, since speed changes in a vehicle are not produced instantaneously [2]:

$$\dot{h}_i = v_{i-1} - v_i \tag{1.3a}$$

$$\dot{v}_i = a_i \tag{1.3b}$$

$$\tau_i \dot{a}_i = -a_i + F_i\left(h_j, v_j, a_j\right), \tag{1.3c}$$

where τ_i is a time constant of the vehicle and $F_i\left(h_j, v_j, a_j\right)$ is a function that represents the acceleration demand, which in general can depend on any net bumper-to-bumper distance h_j, any speed v_j and any acceleration a_j among those corresponding to all vehicles in the setup. This function can be given either by a model of human driving (see Chapter 2) or by the controller of an autonomous vehicle (see Chapters 4 and 5).

Note that the definition of q does not matter yet, since the term L_{i-1} when taking q from the frontal bumpers, or the term L_i when taking q from the rear bumpers, are cancelled when computing $\dot{h}_i$, since those lengths for a single vehicle are constant. However, in Chapter 3, a fleet of vehicles will be modeled as one large vehicle with variable length, therefore the L_{i-1} or L_i term will depend on time and, in general, will not be cancelled when computing $\dot{h}_i$. It is then important to remark that the definition of q does matter only when the length of the fleet is variable.

Chapter 2

Selection of a control-oriented human driving model

One of the first things to do is to select a model for the behaviour of those vehicles which are driven by humans. A couple of well-known models have been tested by means of MATLAB and Simulink. The simulation setup for this chapter is a circular track of $d = 230m$ where 22 human driven vehicles travel, all of them starting at rest and in initial positions such that only the first one has space to accelerate at first (see Figure 2.1, where vehicles travel counterclockwise).

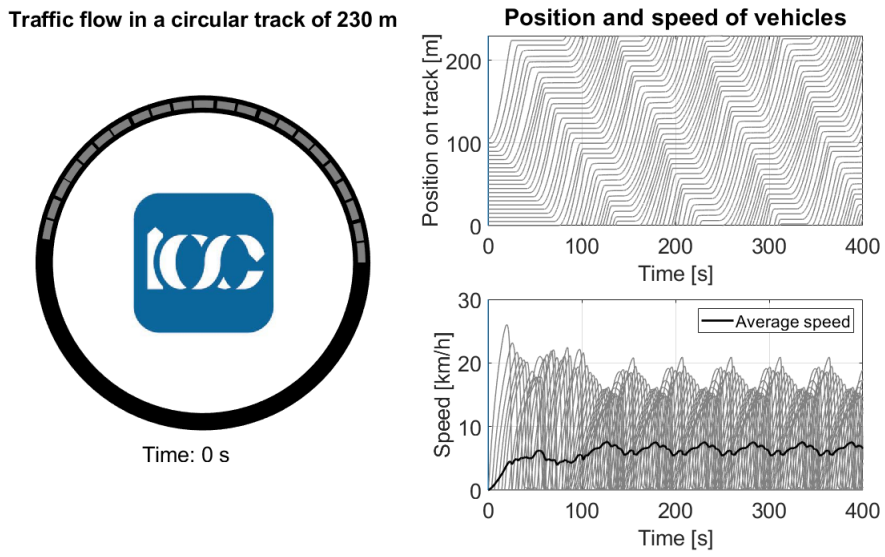

Figure 2.1: Left: setup consisting of a circular track (black) with 22 human driven vehicles (gray) ready to travel counterclockwise. Right: plots of position and speed of each of the human driven vehicles in the track. In this case, SG effect is evident since speed of vehicles indicate sudden acceleration and braking, even including full stops.

One strong condition for choosing one model is that the dynamics must lead to Stop and Go (SG) effect, since that is a characteristic of human driving. Descriptions of both models follow.

2.1 Microscopic Traffic Simulator Model

Consider a classical human driving model: the Microscopic Traffic Simulator (MITSIM or MTS) Model [3].

It presents three different regimes, the main one being the so-called Car Following (CF) regime. Consider the bumper-to-bumper distance, h_i, defined as in (1.1), the speed v_i, the speed of the precedent vehicle v_{i-1} and some constant parameters which are better described in Table 2.1. The acceleration demand for the CF regime reads:

$$F_i^{MTS-CF} = \begin{cases} \alpha^+ \frac{(v_i)^{\beta^+}}{(h_i)^{\gamma^+}} (v_{i-1} - v_i) & \text{if } v_i \leq v_{i-1} \\ \alpha^- \frac{(v_i)^{\beta^-}}{(h_i)^{\gamma^-}} (v_{i-1} - v_i) & \text{if } v_i > v_{i-1}. \end{cases} \tag{2.1}$$

Another regime is the Free Driving (FD) regime, which takes part when the vehicle is unconstrained. It tries to achieve its desired speed v_i^0 following this particular acceleration demand:

$$F_i^{MTS-FD} = \begin{cases} a_i^+ & \text{if } v_i < v_i^0 \\ 0 & \text{if } v_i = v_i^0 \\ a_i^- & \text{if } v_i > v_i^0, \end{cases} \tag{2.2}$$

where all constant parameters are better described in Table 2.1.

Finally, the third regime is the Emergency Braking (EB) regime. Consider the acceleration of the precedent vehicle, a_{i-1}, and other constant parameters which are better described in Table 2.1. When, for any reason, the vehicle is too close to its precedent vehicle, this regime forces a braking in order to avoid an eventual collision:

$$F_i^{MTS-EB} = \begin{cases} \min\left(a_i^-, a_{i-1} - \frac{0.5(v_i - v_{i-1})^2}{h_i}\right) & \text{if } v_i > v_{i-1} \\ \min\left(a_i^-, a_{i-1} + 0.25 a_i^-\right) & \text{if } v_i \leq v_{i-1}. \end{cases} \tag{2.3}$$

But, how to choose in real time which of the three regimes is more adequate for the vehicle? The criterion suggested by [3] is to define a time headway, namely $t_i = h_i/v_i$, and compare it to two thresholds, namely t^+ and t^-. If it is strictly greater than the upper threshold, then the vehicle is considered not to be constrained and it will be

in FD regime. If it is between the two thresholds, including them, then the regime of CF applies. If it is lower than the lower threshold, then the vehicle is considered to be too close and the EB regime applies. With that in mind, and breaking down the $\min$ functions, the full system can be arranged in a single piecewise function:

$$F_i^{MTS} = \begin{cases} a_i^- & \text{if } t_i < t^- \text{ and } v_i > v_{i-1} \text{ and } a_i^- \leq a_{i-1} - \frac{0.5(v_i - v_{i-1})^2}{h_i} \\ a_{i-1} - \frac{0.5(v_i - v_{i-1})^2}{h_i} & \text{if } t_i < t^- \text{ and } v_i > v_{i-1} \text{ and } a_i^- > a_{i-1} - \frac{0.5(v_i - v_{i-1})^2}{h_i} \\ a_i^- & \text{if } t_i < t^- \text{ and } v_i \leq v_{i-1} \text{ and } a_i^- \leq a_{i-1} + 0.25a_i^- \\ a_{i-1} + 0.25a_i^- & \text{if } t_i < t^- \text{ and } v_i \leq v_{i-1} \text{ and } a_i^- > a_{i-1} + 0.25a_i^- \\ \alpha^+ \frac{(v_i)^{\beta^+}}{(h_i)^{\gamma^+}} (v_{i-1} - v_i) & \text{if } t^- \leq t_i \leq t^+ \text{ and } v_i \leq v_{i-1} \\ \alpha^- \frac{(v_i)^{\beta^-}}{(h_i)^{\gamma^-}} (v_{i-1} - v_i) & \text{if } t^- \leq t_i \leq t^+ \text{ and } v_i > v_{i-1} \\ a_i^+ & \text{if } t_i > t^+ \text{ and } v_i < v_i^0 \\ 0 & \text{if } t_i > t^+ \text{ and } v_i = v_i^0 \\ a_i^- & \text{if } t_i > t^+ \text{ and } v_i > v_i^0. \end{cases} \tag{2.4}$$

Lots of parameters are involved. Table 2.1 gathers them up. It is important to remark that all those parameters are generated from a random Gaussian distribution so that, in case of having multiple vehicles, each of them will have different characteristics, thus modeling the fact that vehicles and drivers are different. The mean values of those parameters are taken from those suggested in [3], although the authors of that book do not seem to use any standard deviation.

The biggest problem with this model, from a mathematical point of view, is that when introducing the acceleration demand, $F_i^{MTS}(h_i, v_i, v_{i-1}, a_{i-1})$, into system (1.3), there is not a well-defined equilibrium, since no h^{eq} can be computed for any of the 9 possible regimes presented in (2.4). This will be a key factor when selecting one model, since a mathematical analysis will be required in order for the control to be properly designed.

Using the parameters of Table 2.1, the simulations in the same circular track of $230\ m$ with 22 MITSIM vehicles are portrayed in Figure 2.2 (top).

Table 2.1: Parameters corresponding to MITSIM model.

Description	Parameter	Mean	Standard deviation
Maximum acceleration rate	a_i^+	$4.8\ m/s^2$	30%
Normal deceleration rate	a_i^-	$-8.7\ m/s^2$	30%
Lower time headway threshold	t^-	$0.50\ s$	30%
Upper time headway threshold	t^+	$1.36\ s$	30%
Desired speed	v_i^0	$40\ km/h$	$10\ km/h$
Proportionality factor	α^-	$1.55\ \frac{m^{\left(\gamma^- - \beta^-\right)}}{s^{(1-\beta^-)}}$	30%
Proportionality factor	α^+	$2.15\ \frac{m^{\left(\gamma^+ - \beta^+\right)}}{s^{(1-\beta^+)}}$	30%
Speed exponent	β^-	1.08	30%
Speed exponent	β^+	-1.67	30%
Distance exponent	γ^-	1.65	30%
Distance exponent	γ^+	-0.89	30%

2.2 Intelligent Driver Model

Another well-known model for human driving is the Intelligent Driver Model (IDM) [2]. It is made up of only one equation featuring a $\max$ function, and it is capable of modelling the EB regime and the FD regime besides the CF regime:

$$F_i^{IDM}\left(h_i, v_i, v_{i-1}\right) = a_i^{max}\left(1 - \left(\frac{v_i}{v_i^0}\right)^{\delta_i} - \left(\frac{h_i^*}{h_i}\right)^2\right) \tag{2.5a}$$

$$h_i^* = h_i^0 + \max\left(0, v_i T_i + \frac{v_i\left(v_i - v_{i-1}\right)}{2\sqrt{a_i^{max} b_i^{max}}}\right), \tag{2.5b}$$

where h_i is the bumper-to-bumper distance defined as in (1.1), v_i stands for the speed and v_{i-1} stands for the speed of the precedent vehicle. Again, all the constant parameters are gathered and described in Table 2.2, and their values and standard deviations are borrowed from [2]. Note that, again, all parameters are generated from a Gaussian distribution, for the same reasons explained in the previous section.

Alternatively and more useful, the system (2.5) can be written as a single piecewise function, as in (2.6):

$$F_i^{IDM} = \begin{cases} a_i^{max}\left(1 - \left(\frac{v_i}{v_i^0}\right)^{\delta_i} - \left(\frac{h_i^0}{h_i}\right)^2\right) & \text{R0} \\ a_i^{max}\left(1 - \left(\frac{v_i}{v_i^0}\right)^{\delta_i} - \left(\frac{h_i^0 + v_i T_i + \frac{v_i\left(v_i - v_{i-1}\right)}{2\sqrt{a_i^{max} b_i^{max}}}}{h_i}\right)^2\right) & \text{R1}, \end{cases} \tag{2.6}$$

where Regime 0 (R0) stands for those cases when the $\max$ function at (2.5) takes its first slot and Regime 1 (R1) stands for those cases when the $\max$ function at (2.5) takes its second slot.

Table 2.2: Parameters corresponding to IDM model.

Description	Parameter	Mean	Standard deviation
Maximum acceleration	a_i^{max}	$1\ m/s^2$	$0.2\ m/s^2$
Maximum deceleration	b_i^{max}	$3.5\ m/s^2$	$0.2\ m/s^2$
Minimum net distance	h_i^0	$2\ m$	$0.2\ m$
Safety time headway	T_i	$0.7\ s$	$0.2\ s$
Desired speed	v_i^0	$40\ km/h$	$10\ km/h$
Acceleration exponent	δ_i	0.4	0

Using the parameters of Table 2.2, the results of the simulations in the same circular track of $230\ m$ with 22 IDM vehicles are portrayed in Figure 2.2 (bottom).

2.3 Comparison and selection of a human driving model

So far, two human driving models have been implemented in MATLAB and Simulink, and the results of both simulations are plotted in Figure 2.2.

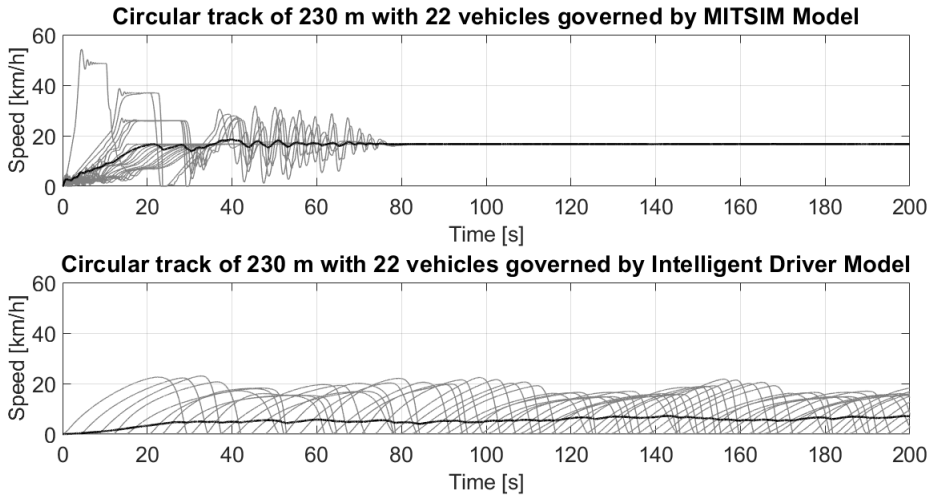

Figure 2.2: Comparison between the results of simulations with 22 MITSIM vehicles (top) and 22 IDM vehicles (bottom) traveling in a circular track of 230 m.

The first one, the MITSIM Model, appears to show some SG effect during the first

seconds, since vehicles increase and decrease suddenly their speeds, but at a point all vehicles stabilize at a constant value. Therefore, at least for this density of vehicles and the set of parameters in Table 2.1 no SG effect is shown, which is negative for a human driving model.

However, the IDM does show almost a perfect SG effect from beginning to end of the simulation. Vehicles punctually reach a speed above the apparent capability of the track, so at a point they are forced to brake, in this case even having to stop completely the vehicle. So, at least for this density of vehicles and the set of parameters in Table 2.2, the IDM represents more accurately a model of human driving in terms of SG effect. Apart from that, it is simpler in terms of mathematical analysis, so probably more suitable as a control-oriented human driving model.

Table 2.3: Comparison between human driving models.

	MITSIM	IDM
Number of regimes	9	2
Well-defined equilibrium point	No, in any regime	Yes, in all 2 regimes
Stop and Go effect	Yes, as a transient	Yes, permanent

A comparison between both human driving models is made in Table 2.3, from which some advantages and disadvantages can be extracted. The conclusions of this Chapter are clear:

- the IDM is simpler than the MITSIM Model,
- a control-oriented mathematical analysis is reachable with IDM, whereas with MITSIM Model would be highly complicated,
- unlike MITSIM Model, the IDM shows permanent SG effect, which fits human driving better.

Definitely, from now on, the human driven vehicles and the unified fleets of human driven vehicles are being governed by IDM, thus discarding MITSIM for the purposes of the upcoming Chapters.

Chapter 3

Model for a unified fleet of human driven vehicles

The most innovative part of this project is probably contained in this Chapter. Here, an approach to drastically simplify the problem of N vehicles is proposed. The idea is to consider a bunch of human driven vehicles as a single piece or pseudo-vehicle, which has a length that varies in time. Ideally, a fleet of n_H human driven vehicles can be reduced to one pseudo-vehicle, thus making the analysis and design of controllers way easier.

3.1 Plausibility model for the length variation of a unified fleet of human driven vehicles

Consider the setup in Figure 3.1, which consists of an autonomous vehicle leading and a unified fleet of human driven vehicles (UFHDV) chasing.

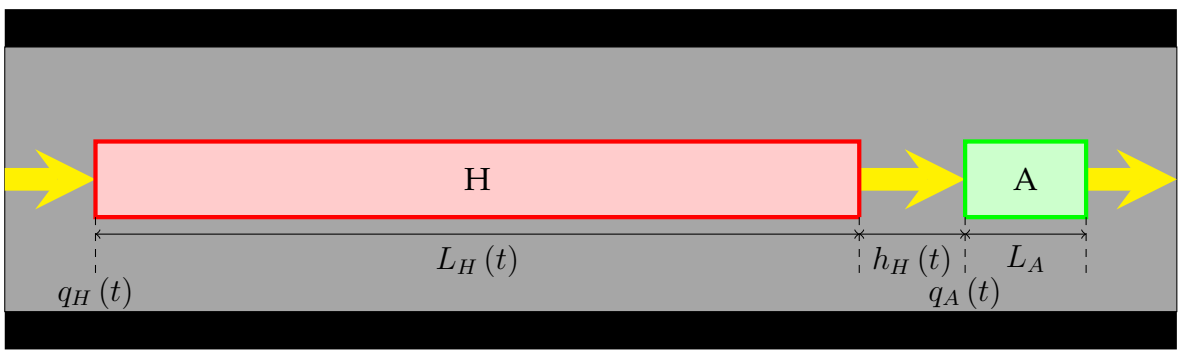

Figure 3.1: One autonomous vehicle leading a UFHDV of variable length.

The net bumper-to-bumper distance h_H may be defined by taking the absolute positions q from the rear bumper of vehicles:

$$h_H = q_A - q_H - L_H, \tag{3.1}$$

where the subscripts H and A refer to UFHDV with variable length and autonomous vehicle, respectively.

Since the length of a fleet of vehicles should fulfill the rule of "the faster they travel, the larger the space they occupy", due to security distance reasons, a plausibility model for the length of a fleet of n_H human driven vehicles is:

$$L_H = \eta_H v_H + \sum_{j=1}^{n_H} l_j, \tag{3.2}$$

with $\eta_H = \sum_{j=1}^{n_H} T_j$, where T_j is the IDM safety time headway of the jth vehicle inside the fleet, $v_H = \dot{q}_H$ is the speed (from the rear point) of the fleet and l_j is the constant length of the jth vehicle inside the fleet. Next is the dynamics for a UFHDV, which is assumed to be governed by IDM as if it was a single vehicle, only with the incorporation of an acceleration term which comes from deriving (3.2) with respect to time:

$$\dot{h}_H = v_A - v_H - \eta_H a_H \tag{3.3a}$$

$$\dot{v}_H = a_H \tag{3.3b}$$

$$\tau_H \dot{a}_H = -a_H + F_H^{IDM}\left(h_H, v_H, v_A\right). \tag{3.3c}$$

3.2 Dynamical system with the control action applied to the acceleration of the autonomous vehicle

The full system describing the autonomous vehicle and the UFHDV reads:

$$\dot{h}_H = v_A - v_H - \eta_H a_H \tag{3.4a}$$

$$\dot{v}_H = a_H \tag{3.4b}$$

$$\dot{a}_H = -\frac{1}{\tau_H} a_H + \frac{1}{\tau_H} F_H^{IDM}\left(h_H, v_H, v_A\right) \tag{3.4c}$$

$$\dot{v}_A = a_A \tag{3.4d}$$

$$\dot{a}_A = -\frac{1}{\tau_A} a_A + \frac{1}{\tau_A} u, \tag{3.4e}$$

where a control u is applied to the acceleration of the autonomous vehicle a_A.

3.3 Equilibrium points and linearization for the open loop system

In order for the controller to be designed, a linearization around the equilibrium point of the system is going to be performed. Since working with IDM, two separate linearizations take part, one for the system staying in R0 and another for the system staying in R1. Note that switches between regimes may occur.

The objective of the control u is to achieve a steady state value of the speed of the UFHDV, $v_H^{eq} = v_r$, where v_r is the reference speed. So, although u is not defined yet, it will be defined such that this condition applies. The other equilibrium points may be computed from (3.4). They are obtained when setting time derivatives equal to zero. It is straightforward, from $\dot{h}_H = \dot{v}_H = \dot{v}_A = \dot{a}_A = 0$, that $v_A^{eq} = v_r$ and $a_H^{eq} = a_A^{eq} = u^{eq} = 0$. Considering separately both regimes of IDM, the whole set of equilibrium points reads, after some calculation:

$$h_H^{eq} = \begin{cases} h_H^0 \left(1 - \left(\frac{v_r}{v_H^0}\right)^{\delta_H}\right)^{-1/2} & \text{R0} \\ (h_H^0 + v_r T_H) \left(1 - \left(\frac{v_r}{v_H^0}\right)^{\delta_H}\right)^{-1/2} & \text{R1} \end{cases} \tag{3.5a}$$

$$v_H^{eq} = v_A^{eq} = v_r \tag{3.5b}$$

$$a_H^{eq} = a_A^{eq} = u^{eq} = 0. \tag{3.5c}$$

Note that, at the equilibrium, the system is necessarily in R1, since for any positive reference speed one has that $\max(0, v_r T_H) = v_r T_H$. This implies that, as long as the system is asymptotically stable, the dynamics will always tend to this R1 equilibrium.

However, the linearization will be done separately for R0 and R1, since in the road to equilibrium the system may switch from one regime to the other an unknown number of times. In other words, the design, mainly done for R1, must guarantee that the system is also stable in R0.

One can find a linearized system which approximates the dynamics around the equilibrium points in (3.5), such that $\dot{\tilde{x}} = A\tilde{x} + B\tilde{u}$, where $\tilde{x} = x - x^{eq}$, with the vector of state variables being $x = \begin{bmatrix} h_H & v_H & a_H & v_A & a_A \end{bmatrix}^T$ and $x^{eq} = \begin{bmatrix} h_H^{eq} & v_H^{eq} & a_H^{eq} & v_A^{eq} & a_A^{eq} \end{bmatrix}^T$; and $\tilde{u} = u - u^{eq}$.

According to theory, the matrix A of the linearized open loop system is computed

as follows [4]:

$$A = \begin{bmatrix} \frac{\partial \dot{h}_H}{\partial h_H} & \frac{\partial \dot{h}_H}{\partial v_H} & \frac{\partial \dot{h}_H}{\partial a_H} & \frac{\partial \dot{h}_H}{\partial v_A} & \frac{\partial \dot{h}_H}{\partial a_A} \\ \frac{\partial \dot{v}_H}{\partial h_H} & \frac{\partial \dot{v}_H}{\partial v_H} & \frac{\partial \dot{v}_H}{\partial a_H} & \frac{\partial \dot{v}_H}{\partial v_A} & \frac{\partial \dot{v}_H}{\partial a_A} \\ \frac{\partial \dot{a}_H}{\partial h_H} & \frac{\partial \dot{a}_H}{\partial v_H} & \frac{\partial \dot{a}_H}{\partial a_H} & \frac{\partial \dot{a}_H}{\partial v_A} & \frac{\partial \dot{a}_H}{\partial a_A} \\ \frac{\partial \dot{v}_A}{\partial h_H} & \frac{\partial \dot{v}_A}{\partial v_H} & \frac{\partial \dot{v}_A}{\partial a_H} & \frac{\partial \dot{v}_A}{\partial v_A} & \frac{\partial \dot{v}_A}{\partial a_A} \\ \frac{\partial \dot{a}_A}{\partial h_H} & \frac{\partial \dot{a}_A}{\partial v_H} & \frac{\partial \dot{a}_A}{\partial a_H} & \frac{\partial \dot{a}_A}{\partial v_A} & \frac{\partial \dot{a}_A}{\partial a_A} \end{bmatrix}_{eq} = \begin{bmatrix} 0 & -1 & -\eta_H & 1 & 0 \\ 0 & 0 & 1 & 0 & 0 \\ A_{3,1} & A_{3,2} & -\frac{1}{\tau_H} & A_{3,4} & 0 \\ 0 & 0 & 0 & 0 & 1 \\ 0 & 0 & 0 & 0 & -\frac{1}{\tau_A} \end{bmatrix}, \tag{3.6}$$

where

$$A_{3,1} = \left[\frac{\partial \dot{a}_H}{\partial h_H}\right]_{eq} = \begin{cases} \frac{2a_H^{max}}{\tau_H h_H^0}\left(1 - \left(\frac{v_r}{v_H^0}\right)^{\delta_H}\right)^{3/2} & \text{R0} \\ \frac{2a_H^{max}}{\tau_H\left(h_H^0 + v_r T_H\right)}\left(1 - \left(\frac{v_r}{v_H^0}\right)^{\delta_H}\right)^{3/2} & \text{R1} \end{cases} \tag{3.7a}$$

$$A_{3,2} = \left[\frac{\partial \dot{a}_H}{\partial v_H}\right]_{eq} = \begin{cases} -\frac{a_H^{max}}{\tau_H}\frac{\delta_H (v_r)^{\delta_H - 1}}{\left(v_H^0\right)^{\delta_H}} & \text{R0} \\ -\frac{a_H^{max}}{\tau_H}\left(\frac{\delta_H (v_r)^{\delta_H - 1}}{\left(v_H^0\right)^{\delta_H}} + \frac{v_r + 2T_H\sqrt{a_H^{max} b_H^{max}}}{\left(h_H^0 + v_r T_H\right)\sqrt{a_H^{max} b_H^{max}}}\left(1 - \left(\frac{v_r}{v_H^0}\right)^{\delta_H}\right)\right) & \text{R1} \end{cases} \tag{3.7b}$$

$$A_{3,4} = \left[\frac{\partial \dot{a}_H}{\partial v_A}\right]_{eq} = \begin{cases} 0 & \text{R0} \\ \frac{a_H^{max} v_r}{\tau_H\sqrt{a_H^{max} b_H^{max}}\left(h_H^0 + v_r T_H\right)}\left(1 - \left(\frac{v_r}{v_H^0}\right)^{\delta_H}\right) & \text{R1.} \end{cases} \tag{3.7c}$$

Matrix B of the linearized open loop system is given by

$$B = \begin{bmatrix} \frac{\partial \dot{h}_H}{\partial u} & \frac{\partial \dot{v}_H}{\partial u} & \frac{\partial \dot{a}_H}{\partial u} & \frac{\partial \dot{v}_A}{\partial u} & \frac{\partial \dot{a}_A}{\partial u} \end{bmatrix}_{eq}^T = \begin{bmatrix} 0 & 0 & 0 & 0 & \frac{1}{\tau_A} \end{bmatrix}^T. \tag{3.8}$$

3.4 Transfer function of the open loop system

It is often useful to explicitly compute the transfer function in order to gain an insight of the system. The dynamics of the open loop system are given by:

$$\dot{x}(t) = Ax(t) + Bu(t). \tag{3.9}$$

Now, using the Laplace transform one gets:

$$sIX(s) = AX(s) + BU(s); \tag{3.10}$$

then, rearranging terms and isolating one can obtain the expression for the transformed state vector:

$$X(s) = (sI - A)^{-1} BU(s). \tag{3.11}$$

Finally, substituting the transformed state vector into the expression of the output yields:

$$Y(s) = CX(s) = C(sI - A)^{-1} BU(s). \tag{3.12}$$

The transfer function $G(s)$ is computed from the ratio of the output $Y(s)$ with respect to the input $U(s)$ as follows:

$$G(s) = \frac{Y(s)}{U(s)} = C(sI - A)^{-1} B, \tag{3.13}$$

which, in explicit form, reads as:

$$G(s) = \frac{1}{\tau_A} \frac{A_{3,4}s + A_{3,1}}{s^5 + p_4 s^4 + p_3 s^3 + p_2 s^2 + p_1 s}, \tag{3.14}$$

where the coefficients are given by

$$p_4 = \frac{1}{\tau_H} + \frac{1}{\tau_A} \tag{3.15a}$$

$$p_3 = \frac{1}{\tau_H \tau_A} + \eta_H A_{3,1} - A_{3,2} \tag{3.15b}$$

$$p_2 = \frac{\tau_A + \eta_H}{\tau_A} A_{3,1} - \frac{1}{\tau_A} A_{3,2} \tag{3.15c}$$

$$p_1 = \frac{1}{\tau_A} A_{3,1}. \tag{3.15d}$$

Note that a pure integrator is part of the open loop system, since a term $1/s$ is common factor of the transfer function. This ensures that no additional integral action is required in the controller in order to ensure zero steady state error in the system when the reference v_r is constant. However, in case v_r takes the form of a ramp, additional integral action is needed in order for zero steady state error to arise.

Chapter 4

Control of a unified fleet of human driven vehicles by means of autonomous vehicles: full state feedback with integral action

Once the open loop model of a UFHDV with variable length has been completely defined and even linearized in Chapter 3, it is time to design the control u. At first, it will be chosen to be a full state feedback controller with integral action [4][5], of the form (4.1):

$$u = -k_1 h_H - k_2 v_H - k_3 a_H - k_4 v_A - k_5 a_A - k_z z \tag{4.1a}$$

$$\dot{z} = v_H - v_r, \tag{4.1b}$$

where k_i ($i = 1, ..., 5, z.$) are the gains to be designed, z is the integral action and v_r is the reference speed for v_H. Notice that, at equilibrium, $v_H^{eq} = v_r$ since $\dot{z} = 0$, thus fulfilling the only condition stated in Chapter 3 for the control u.

Given that the open loop system dynamics (3.14) already contain a pure integrator, the additional integral action allows zero steady state error not only for a constant desired speed value, but also for ramp speed references in case they are used.

The complete scheme of the state feedback controller with integral action is drawn in Figure 4, from which it is going to be implemented in Simulink.

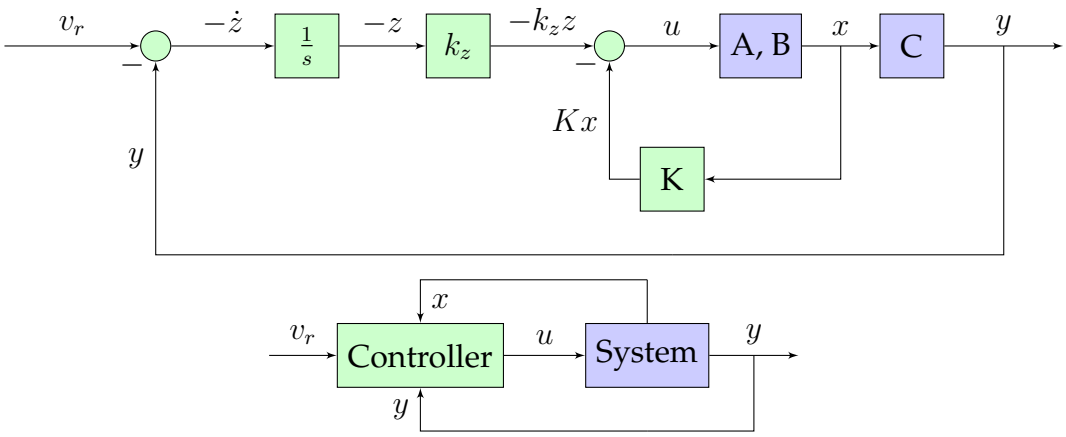

Figure 4.1: Linear system featuring a full state feedback controller with integral action. Green blocks correspond to the controller and blue blocks correspond to the process.

4.1 Closed loop system

From now on, consider the augmented system, where the integral action is included in the augmented state vector. The state feedback control with integral action takes the following matrix form [4][5]:

$$u = -\left[\begin{array}{c:c} K & k_z \end{array}\right] \left[\begin{array}{c} x \\ \hdashline z \end{array}\right], \tag{4.2}$$

$K = \begin{bmatrix} k_1 & k_2 & k_3 & k_4 & k_5 \end{bmatrix}$ being the matrix of gains and z being the integral action, which is related with the integral of $\dot{z} = v_H - v_r$.

Now compute the matrix A_{CL}, which corresponds to the closed loop linearized system (4.3) and takes the integral action into account. Its eigenvalues will be crucial for the stability, as well as settling time and overshoot of the closed loop system [4][5]. The closed loop augmented system takes the following matrix form:

$$\left[\begin{array}{c} \dot{x} \\ \hdashline \dot{z} \end{array}\right] = A_{CL} \left[\begin{array}{c} x \\ \hdashline z \end{array}\right] + B_{CL} v_r \tag{4.3a}$$

$$y = C_{CL} \left[\begin{array}{c} x \\ \hdashline z \end{array}\right], \tag{4.3b}$$

where the closed loop matrices are written as:

$$A_{CL} = \left[\begin{array}{c:c} A - BK & -k_z B \\ \hdashline C & 0 \end{array}\right] \tag{4.4a}$$

$$C_{CL} = \left[\begin{array}{c:c} C & 0 \end{array}\right]. \tag{4.4b}$$

So, in explicit form, they read as:

$$A_{CL} = \left[\begin{array}{ccccc:c} 0 & -1 & -\eta_H & 1 & 0 & 0 \\ 0 & 0 & 1 & 0 & 0 & 0 \\ A_{3,1} & A_{3,2} & -\frac{1}{\tau_H} & A_{3,4} & 0 & 0 \\ 0 & 0 & 0 & 0 & 1 & 0 \\ -\frac{k_1}{\tau_A} & -\frac{k_2}{\tau_A} & -\frac{k_3}{\tau_A} & -\frac{k_4}{\tau_A} & -\frac{k_5+1}{\tau_A} & -\frac{k_z}{\tau_A} \\ \hdashline 0 & 1 & 0 & 0 & 0 & 0 \end{array}\right] \tag{4.5a}$$

$$B_{CL} = \left[\begin{array}{ccccc:c} 0 & 0 & 0 & 0 & 0 & -1 \end{array}\right]^T \tag{4.5b}$$

$$C_{CL} = \left[\begin{array}{ccccc:c} 0 & 1 & 0 & 0 & 0 & 0 \end{array}\right]. \tag{4.5c}$$

4.2 Transfer function of the closed loop system

The reference value for the output $y = v_H$ is $y^{eq} = v_r$; in other words, the closed loop system consists of an input v_r and an output v_H. The transfer function of the linearized system is going to be computed from (4.3) and (4.4). First, consider the augmented dynamical system:

$$\left[\begin{array}{c} \dot{x}(t) \\ \hdashline \dot{z}(t) \end{array}\right] = \left[\begin{array}{c:c} A - BK & -k_z B \\ \hdashline C & 0 \end{array}\right] \left[\begin{array}{c} x(t) \\ \hdashline z(t) \end{array}\right] + \left[\begin{array}{c} \emptyset \\ \hdashline -1 \end{array}\right] v_r(t). \tag{4.6}$$

Now, using the Laplace transform one gets:

$$sI \left[\begin{array}{c} X(s) \\ \hdashline Z(s) \end{array}\right] = \left[\begin{array}{c:c} A - BK & -k_z B \\ \hdashline C & 0 \end{array}\right] \left[\begin{array}{c} X(s) \\ \hdashline Z(s) \end{array}\right] + \left[\begin{array}{c} \emptyset \\ \hdashline -1 \end{array}\right] V_r(s); \tag{4.7}$$

then, rearranging terms and isolating one can obtain the expression for the transformed state vector:

$$\left[\begin{array}{c} X(s) \\ \hdashline Z(s) \end{array}\right] = \left[\begin{array}{c:c} sI - A + BK & k_z B \\ \hdashline -C & s \end{array}\right]^{-1} \left[\begin{array}{c} \emptyset \\ \hdashline -1 \end{array}\right] V_r(s). \tag{4.8}$$

Finally, substituting the transformed state vector into the expression of the output yields:

$$Y(s) = C_{CL} \left[\begin{array}{c} X(s) \\ \hdashline Z(s) \end{array}\right] = C_{CL} \left[\begin{array}{c:c} sI - A + BK & k_z B \\ \hdashline -C & s \end{array}\right]^{-1} \left[\begin{array}{c} \emptyset \\ \hdashline -1 \end{array}\right] V_r(s). \tag{4.9}$$

The transfer function $G(s)$ is computed from the ratio of the output $Y(s)$ with respect to the input $V_r(s)$ as follows:

$$G(s) = \frac{Y(s)}{V_r(s)} = C_{CL} \left[\begin{array}{c:c} sI - A + BK & k_z B \\ \hdashline -C & s \end{array}\right]^{-1} \left[\begin{array}{c} \emptyset \\ \hdashline -1 \end{array}\right], \tag{4.10}$$

which, in explicit form, reads as:

$$G(s) = \frac{k_z}{\tau_A} \frac{A_{3,4}s + A_{3,1}}{s^6 + p_5 s^5 + p_4 s^4 + p_3 s^3 + p_2 s^2 + p_1 s + p_0}, \tag{4.11}$$

where the coefficients are given by

$$p_5 = \frac{1}{\tau_H} + \frac{k_5 + 1}{\tau_A} \tag{4.12a}$$

$$p_4 = \frac{k_4\tau_H + k_5 + 1}{\tau_H \tau_A} + \eta_H A_{3,1} - A_{3,2} \tag{4.12b}$$

$$p_3 = \frac{k_1\tau_H + k_4}{\tau_H \tau_A} + \left(1 + \eta_H \frac{k_5 + 1}{\tau_A}\right) A_{3,1} - \frac{k_5 + 1}{\tau_A} A_{3,2} + \frac{k_3}{\tau_A} A_{3,4} \tag{4.12c}$$

$$p_2 = \frac{k_1}{\tau_H \tau_A} + \frac{k_3 + \eta_H k_4 + k_5 + 1}{\tau_A} A_{3,1} - \frac{k_4}{\tau_A} A_{3,2} + \frac{k_2 - \eta_H k_1}{\tau_A} A_{3,4} \tag{4.12d}$$

$$p_1 = \frac{k_2 + k_4}{\tau_A} A_{3,1} - \frac{k_1}{\tau_A} A_{3,2} + \frac{k_z - k_1}{\tau_A} A_{3,4} \tag{4.12e}$$

$$p_0 = \frac{k_z}{\tau_A} A_{3,1}. \tag{4.12f}$$

One can check that the zero frequency gain $G(0) = 1$, thus ensuring that the steady state value of the output $y = v_H$ will equal the value of the step input reference v_r. Regarding the number of poles, this transfer function features 6 poles, which was expected since this is a 5th order system featuring one equation corresponding to an integrator, which adds one extra pole. In general those 6 poles will be located in different places depending on IDM's Regime, but the design will be preferably made considering Regime 1, since that is the regime towards which the system tends in steady state.

Note that in Regime 0, since $A_{3,4} = 0$, there are no zeros at all. However, at Regime 1, since $A_{3,4} \neq 0$, one zero appears. This may have an effect resulting in an increase of the overshoot [4].

The zero for Regime 1 is located at:

$$z_1 = -\frac{A_{3,1}}{A_{3,4}} = -\frac{2\sqrt{a_H^{max} b_H^{max}}}{v_r} \left(1 - \left(\frac{v_r}{v_H^0}\right)^{\delta_H}\right)^{1/2}. \tag{4.13}$$

Given that the reference v_r will usually be smaller than IDM's desired speed v_H^0, then this zero will be real and it will be located in the left half complex plane, thus

preventing the system from being nonminimum phase and exhibiting undershoot. The system is therefore expected to only exhibit overshoot.

Now it is time to design the gain factors by means of Ackermann's formula in order for the eigenvalues/poles to be placed properly. Note that there are 2 transfer functions, each corresponding to a different IDM regime, but the design will be made considering only Regime 1 for the aforementioned reasons. So there will 6 poles to be allocated and 1 zero.

4.3 Pole allocation

The first hypothesis for this section is to consider that the design can be done for 2 dominant poles forming one pair of complex conjugate poles (as if it was a second order system) and the remaining 4 poles will have a real part of more that five times the real part of the dominant pair, thus making them negligible with respect to the dominant pair [4][5].

Consider a second order system with a transfer function of the form (4.14):

$$G(s) = \frac{k{\omega_0}^2}{s^2 + 2\zeta\omega_0 s + {\omega_0}^2}. \tag{4.14}$$

Its eigenvalues/poles are given by:

$$\lambda_1 = -\zeta\omega_0 + \sqrt{{\omega_0}^2\left(\zeta^2 - 1\right)} = -\sigma + j\omega_d \tag{4.15a}$$

$$\lambda_2 = -\zeta\omega_0 - \sqrt{{\omega_0}^2\left(\zeta^2 - 1\right)} = -\sigma - j\omega_d, \tag{4.15b}$$

where $\sigma = \zeta\omega_0$ is the damping factor and $\omega_d = \omega_0\sqrt{1-\zeta^2}$ is the damping frequency. The damping coefficient ζ plays an essential role: if $\zeta = 0$ the system is an oscillator, if $0 < \zeta < 1$ the system is underdamped, if $\zeta = 1$ the system is critically damped, if $\zeta > 1$ the system is overdamped [4].

The case of interest is the underdamped system, for which $0 < \zeta < 1$. From it the rise time (T_r), the 2%-settling time (T_s) and the maximum overshoot (M_p) can be

approximately obtained [4]. They are respectively given by:

$$T_r \approx \frac{1}{\omega_0} \exp\left(\frac{\psi}{\tan\psi}\right) \tag{4.16a}$$

$$\psi = \arctan\left(\frac{\sqrt{1-\zeta^2}}{\zeta}\right) \tag{4.16b}$$

$$T_s \approx \frac{4}{\sigma} \tag{4.16c}$$

$$M_p \approx \exp\left(-\frac{\pi\sigma}{\omega_d}\right). \tag{4.16d}$$

Certain values of the 2%-settling time and maximum overshoot are desired, therefore the real and imaginary parts of the dominant pair depend on T_s and M_p. In other words, specific values for 2%-settling time and maximum overshoot are going to be chosen, and from them the location of the dominant pair of poles will arise. The remaining 4 poles are going to be dominated. One valid set of poles may be be allocated, for instance, this way:

$$\lambda_1 = -\sigma + j\omega_d \tag{4.17a}$$

$$\lambda_2 = -\sigma - j\omega_d \tag{4.17b}$$

$$\lambda_3 = -21\sigma \tag{4.17c}$$

$$\lambda_4 = -22\sigma \tag{4.17d}$$

$$\lambda_5 = -23\sigma \tag{4.17e}$$

$$\lambda_6 = -24\sigma, \tag{4.17f}$$

where σ and ω_d depend on T_s and M_p as already seen:

$$\sigma = \frac{4}{T_s} \tag{4.18a}$$

$$\omega_d = -\frac{\pi\sigma}{\log M_p}. \tag{4.18b}$$

Thus, the behaviour of the 6th order system with eigenvalues λ_1, λ_2, λ_3, λ_4, λ_5, λ_6 will be very similar to the behaviour of a 2nd order system with eigenvalues λ_1, λ_2.

In order to compute the gains by means of Ackermann's formula, consider again the augmented system dynamics [5]:

$$\begin{bmatrix} \dot{x}(t) \\ \hdashline \dot{z}(t) \end{bmatrix} = A_K \begin{bmatrix} x(t) \\ \hdashline z(t) \end{bmatrix} + B_K u(t) + \begin{bmatrix} \emptyset \\ \hdashline -1 \end{bmatrix} v_r(t), \tag{4.19}$$

with

$$A_K = \left[\begin{array}{c:c} A & \emptyset \\ \hdashline C & 0 \end{array}\right] \tag{4.20a}$$

$$B_K = \left[\begin{array}{c} B \\ \hdashline 0 \end{array}\right]. \tag{4.20b}$$

Recall that the control law $u(t)$ takes the form (4.2), which shall be seen as a full state feedback on the augmented state vector corresponding to (4.19). So those 6 gains, which include the integral action gain, will be computed by means of Ackermann's formula:

$$\left[\begin{array}{c:c} K & k_z \end{array}\right] = \begin{bmatrix} 0 & 0 & 0 & 0 & 0 & 1 \end{bmatrix} {W_C}^{-1} P_d(A_K), \tag{4.21}$$

where W_C is the controllability (or Kalman) matrix, which will be numerically proven to be full rank, this is, rank 6, in order for the system to be controllable [4]:

$$W_C = \left[\begin{array}{c:c:c:c:c:c} B_K & A_K B_K & {A_K}^2 B_K & {A_K}^3 B_K & {A_K}^4 B_K & {A_K}^5 B_K \end{array}\right]. \tag{4.22}$$

In turn, $P_d(A_K)$ is the desired characteristic polynomial whose roots are the desired poles of the system evaluated in the matrix A_K [4]:

$$P_d(A_K) = (A_K - \lambda_1 I)(A_K - \lambda_2 I)(A_K - \lambda_3 I)(A_K - \lambda_4 I)(A_K - \lambda_5 I)(A_K - \lambda_6 I). \tag{4.23}$$

The calculation of those gains is carried out using MATLAB.

4.4 Switching between IDM's regimes

The design has been made assuming the system is permanently in R1. Obviously, every combination of v_r and T_s yield the desired behaviour as long as the system remains in R1; however, with that design and the system switching to R0, everything could happen.

As it can be seen in Figure 4.2, not every combination of v_r and T_s works. So, when designing, one must choose a combination of v_r and T_s within the blue areas, just in case the system eventually switches to Regime 0, in order for it not to be unstable.

It is worth mentioning that the positions of the dominated poles (4.17) do affect the shape of the stability regions in Figure 4.2. The values chosen here were among the best possible combinations of dominated poles in terms of stability.

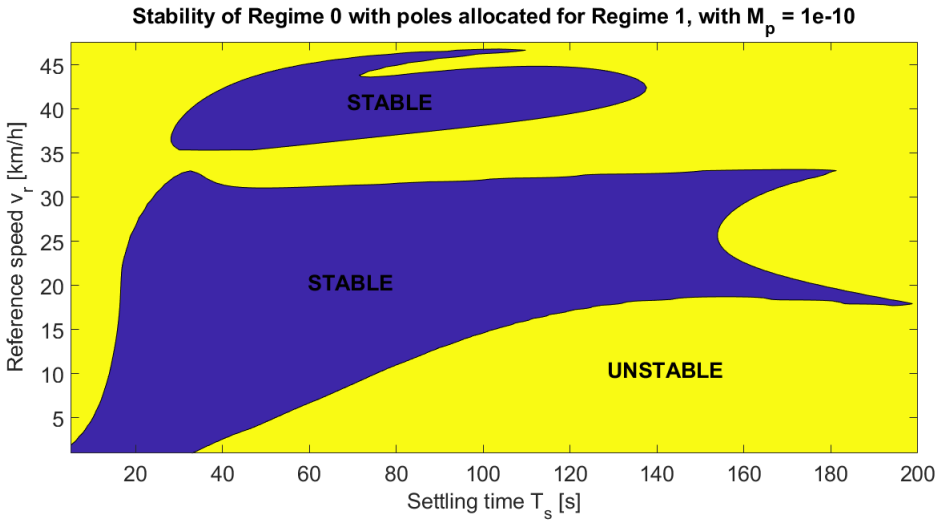

Figure 4.2: Regions of stability of IDM's Regime 0 with the design corresponding to Regime 1, as a function of T_s and v_r. Colour blue indicates stability and colour yellow indicates instability.

4.5 Gain scheduling

In general, the system will not be working for one constant value of v_r. Instead, it is expected to receive a reference value v_r in real time, which can vary in steps, and from it perform the design. Instead of designing the gain factors once and let them remain invariant, gain scheduling is programmed. This means that Ackermann's formula is used at every single change of v_r, thus ensuring proper values of gains continuously and ensuring that poles are always located such that they accomplish the desired settling time and overshoot.

Note that v_r is not treated as a general single time-dependent function, since the theory used in this project does not support time-varying gains; but as a piecewise-defined function with constant steps sufficiently long so that permanent regime is reached before updating the reference v_r.

The idea is, thanks to some optimizer, choose the best value of v_r according to traffic conditions at each moment. This is, however, out of the scope of this project. Figure 4.3 shows the results of using gain scheduling and varying manually the reference v_r in arbitrarily chosen steps.

The output v_H achieves the reference v_r within the required time and overshoot, except for one particular case where the system switches from Regime 1 to Regime 0, although it gets back again to Regime 1. Relatively good news is that, in the switching

case, the system remains stable since the settling time, picked from Figure 4.2, makes Regime 0 be stable for all the values of v_r picked in Figure 4.3. However, neither the settling time nor the overshoot are those desired, since the design for those was made regarding Regime 1.

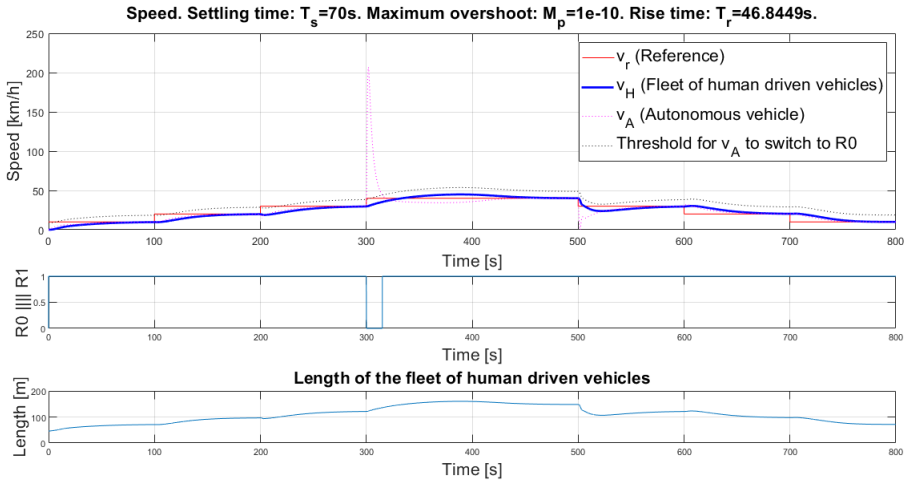

Figure 4.3: Behaviour of the system when designing for $T_s = 70\ s$, $M_p = 10^{-10}$ and a reference speed v_r which varies arbitrarily in steps.

4.6 Numerical validation in a realistic model

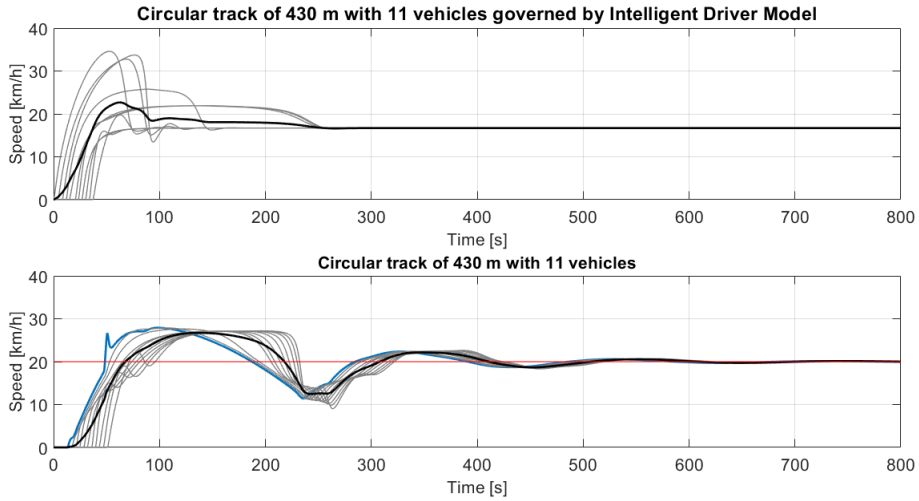

Figure 4.4: Numerical simulation of the full state feedback controller designed in Chapter 4 in a circular track (bottom) and IDM behaviour for the same characteristics in the same track (top).

After the design is made and the model works properly it is time to try to incorporate those controllers in the circular track. The results can be seen in Figure 4.4 (bottom) along with the same setup but only with IDM vehicles (top).

Results are not so good. Indeed, when adding those autonomous vehicles to the track, traffic flow seems to get even worse than with only human drivers. Apparently, autonomous vehicles produce even more SG effect than the human driven ones alone.

This may be due to discrepancies between the model for a UFHDV with variable length and the actual behaviour of separate vehicles in terms of delay. More insight about this is given in Chapter 5.

Chapter 5

Alternative approach: addition of delay and simplification of the controller

After proving that the full state feedback controller with integral action did not perform well in the realistic simulations, some alternatives are necessary, at least for trying to spot mistakes. A simple control that comes to mind is an output feedback proportional controller:

$$u = k\left(v_r - v_H\right), \tag{5.1}$$

being k the gain, v_r the reference speed and v_H the speed of the last vehicle of the fleet. Note that, since $u^{eq} = 0$ (see Chapter 3), the condition that $v_H^{eq} = v_r$ is fulfilled, so this controller is perfectly valid and consistent with the system.

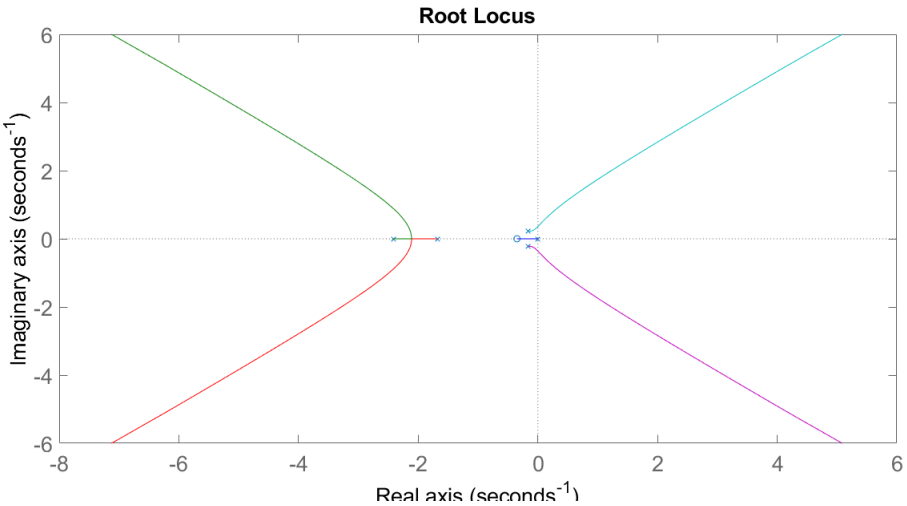

Figure 5.1: Root locus for the proportional controller. Poles are marked with crosses and zeros are marked with circles. The variation of the gain k makes the location of the poles change accordingly, following the respective color lines.

The stability analysis for the proportional controller is simple and is made by means of a root locus (see Figure 5.1), which is useful for choosing an order of magnitude for k that leads to a system, at least, stable. Then, it is a matter of trying some different values and seeing which gives the best dynamical behaviour. After some tries, the value chosen for the following sections is $k = 0.02s^{-1}$. With this controller, no sophisticated design can be made.

5.1 Transfer function of the closed loop system

In order to compute the transfer function, write the dynamical equations, which in matrix form read:

$$\dot{x}(t) = (A - kBC)\, x(t) + kBv_r(t). \tag{5.2}$$

Now, using the Laplace transform one gets:

$$sIX(s) = (A - kBC)\, X(s) + kBV_r(s); \tag{5.3}$$

then, rearranging terms and isolating one can obtain the expression for the transformed state vector:

$$X(s) = k(sI - A + kBC)^{-1} BV_r(s). \tag{5.4}$$

Finally, substituting the transformed state vector into the expression of the output yields:

$$Y(s) = C_{CL}X(s) = kC_{CL}(sI - A + kBC)^{-1} BV_r(s). \tag{5.5}$$

The transfer function $G(s)$ is computed from the ratio of the output $Y(s)$ with respect to the input $V_r(s)$ as follows:

$$G(s) = \frac{Y(s)}{V_r(s)} = kC_{CL}(sI - A + kBC)^{-1} B, \tag{5.6}$$

which, in explicit form, reads as:

$$G(s) = \frac{k}{\tau_A} \frac{A_{3,4}s + A_{3,1}}{s^5 + p_4 s^4 + p_3 s^3 + p_2 s^2 + p_1 s + p_0}, \tag{5.7}$$

where the coefficients are given by

$$p_4 = \frac{1}{\tau_H} + \frac{1}{\tau_A} \tag{5.8a}$$

$$p_3 = \frac{1}{\tau_H \tau_A} + \eta_H A_{3,1} - A_{3,2} \tag{5.8b}$$

$$p_2 = \frac{\tau_A + \eta_H}{\tau_A} A_{3,1} - \frac{1}{\tau_A} A_{3,2} \tag{5.8c}$$

$$p_1 = \frac{1}{\tau_A} A_{3,1} + \frac{k}{\tau_A} A_{3,4} \tag{5.8d}$$

$$p_0 = \frac{k}{\tau_A} A_{3,1}. \tag{5.8e}$$

Again, the zero frequency gain $G(0) = 1$, so the steady state value of the output $y = v_H$ will equal the value of the step input reference v_r, which makes controller (5.1) a consistent one.

5.2 Validation of the UFHDV model

After having the control designed, and now using exclusively the proportional controller, which clearly works better than the integral one, one can perform a comparison regarding the model of a fleet of human driven vehicles with variable length versus the actual implementation where human driven vehicles work as separate units. This will give an insight of how accurate was the approximation model at (3.2).

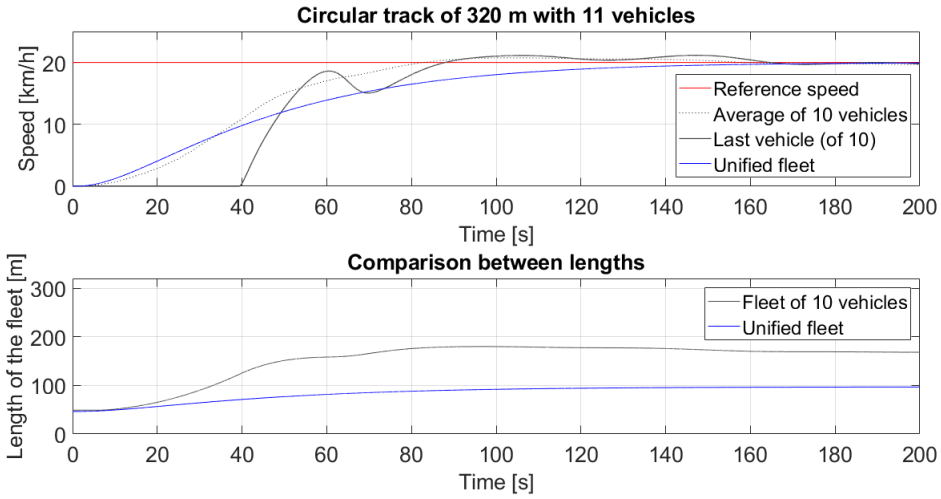

Figure 5.2: Comparison between speeds (top) and length of fleets (bottom) for both the plausibility model and the actual implementation.

The results are shown in Figure 5.2. Two main issues appear. On the one hand, one realizes that the speed (top), although it settles at reference in a reasonable time,

has a considerable delay in the first seconds. In particular, for this fleet of 10 human driven vehicles, the delay is roughly 40 seconds. This can be easily explained since the last vehicle cannot accelerate until its precedent vehicle has moved and opened a gap, which in turn has to wait for its precedent vehicle to move, etc. One thing which is interesting is that the average speed of the 10 separate vehicles has the same approximate shape as the speed of the plausibility model, not showing any delay.

On the other hand, the length of the fleet, although it is true that grows with the speed, it does so in a different way. A quick solution may be replace η_H by approximately $2.5\eta_H$ in (3.2), at least for this particular configuration of 10 vehicles. This way, the final value of the length in the plausibility model would be very similar to the actual one when considering separate vehicles.

So, conclusions from the plausibility model stated at (3.2) are:

1. The speed of the last vehicle in the fleet does not exactly fit the model. Possible improvements are:

   (a) Add a delay to the speed (of the rear point) of the fleet, in order for it to actually behave like the speed (of the rear point) of the fleet and not like the average speed of the fleet. The delay could be expressed as a multiplying transfer function of the type $G_D(s) = e^{-T_D s}$, where the order of magnitude of the time constant seems to depend on the number of vehicles in the fleet and it may be given by $T_D \approx 4n_H$, although further study is needed on this.

   (b) Consider the average speed instead of the speed (of the rear point) of the fleet. This would complicate the starting model and (3.1) and (3.3) would be inconsistent.

2. The length of the fleet does not fit the model by a proportionality factor. Some improvement should be:

   (a) Add a multiplying constant to the speed term in (3.2).

5.3 Comparison between proportional controller and full state feedback controller with integral action

Once the proportional controller is designed and works, it is time to compare it. The difference between the full state feedback controller with integral action (bottom)

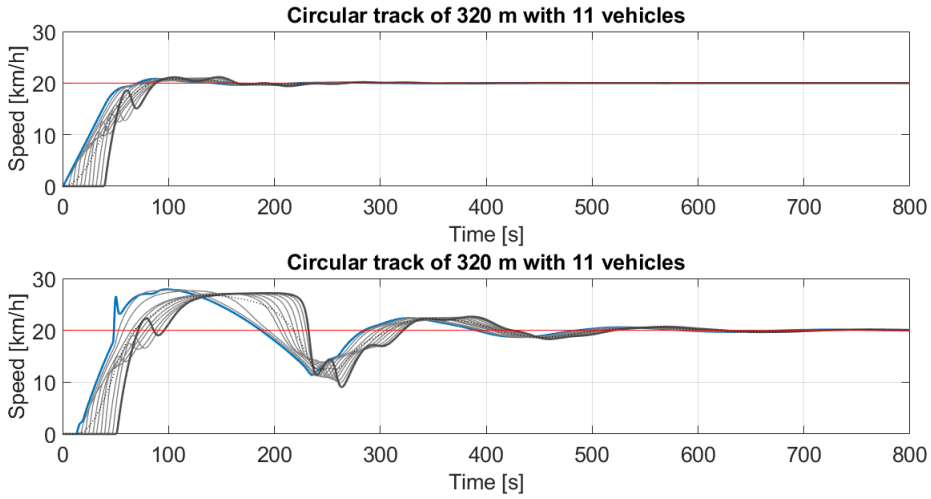

Figure 5.3: Behaviour of the system with a reference speed of $v_r = 20km/h$ in a track of $d = 320m$, with a proportional controller (top) and the full state feedback controller with integral action previously designed (bottom).

and a simple proportional controller of the type (5.1), with $k = 0.02s^{-1}$ (top), can be spotted in Figure 5.3. The state feedback controller with integral action did not work as expected, perhaps due to dissimilarities from the UFHDV with variable length to the actual setup of separate vehicles. Since the UFHDV reacts instantaneously, the model is likely to differ from the actual setup where the last vehicle has to wait for all its precedent vehicles to move before accelerating itself. This effect can be clearly seen in Figure 5.2, where the last vehicle has a delay of about $40s$ with respect to the immediate acceleration of the model of the unified fleet of human driven vehicles.

It is obvious that some things need to be fixed in order for the design to make sense. One important decision for the structure of the project has to be made, and the most important mistake to fix is the type of control used. Although it seemed useful at first sight, the natural appearance of an integrator in the open loop function of the system (see (3.14)) and the incompatibility of the integral action with the delay of the system with respect to the design (see Figure 5.3) make the integral action dispensable.

As it is seems better in Figure 5.3, the simple proportional controller will be the one to be used in Chapter 6. The biggest difference with respect to a state feedback controller is that here no design can be made, this is, there is no option of fixing a settling time and an overshoot directly. Other changes to the model of the fleet of human driven vehicles with variable length, although should be made, are not necessary for accomplishing the objectives of this project.

Chapter 6

Simulation results of traffic flow controlled by autonomous vehicles

After the analysis carried out in Chapters 4 and 5, it is time to finally test the controller-equipped autonomous vehicles in traffic flow within a more realistic ensemble: the circular track.

6.1 Safety braking system

First, some preliminaries are required. Notice that in any previous Chapter did the autonomous vehicle have any limitation. This is, since the designs were made outside the circular track, the autonomous vehicle had absolutely nothing ahead of it, and it could accelerate infinitely and would never crash with another vehicle.

In this Chapter, however, vehicles are traveling within a circular track, which in particular means that autonomous vehicles, as they are designed, risk hitting their precedent vehicle. In order to avoid that, an artificial safety braking term must be added to the control action (5.1), which now reads:

$$u = k\left(v_r - v_H\right) - \frac{0.1}{h_A}, \tag{6.1}$$

where k is the gain of the controller, v_r is the reference speed, v_H is the speed of the last vehicle within the chasing fleet, 0.1 is an arbitrary constant that has been proved to work well and h_A is the bumper-to-bumper distance between the autonomous vehicle and the last vehicle of the other fleet.

This new term will not affect the design when the bumper-to-bumper distance between the autonomous vehicle and its precedent vehicle, h_A, is large enough; however,

it will act as an emergency braking term for limiting the progress of the autonomous vehicle when it is at a considerably low distance from its precedent vehicle. Furthermore, the smoothness of this function allows the autonomous vehicle to start decelerating in advance, thus avoiding severe braking situations that could result in SG effect and may arise if the barrier term were a not so smooth function like $\propto h_A^{-2}$ or $\propto h_A^{-4}$.

6.2 Incorporation of one controller-equipped autonomous vehicle ahead of a fleet of human driven vehicles

The first test's setup will consist of one autonomous vehicle leading a fleet of human driven vehicles. This is unreal since without another autonomous vehicle the speed of the last vehicle in the fleet of human driven vehicles, which is a state variable of the system, is impossible to collect.

So, as it can be visualized in Figure 6.1, one autonomous vehicle equipped with the controller in (6.1) is chased by 10 individual vehicles governed by IDM.

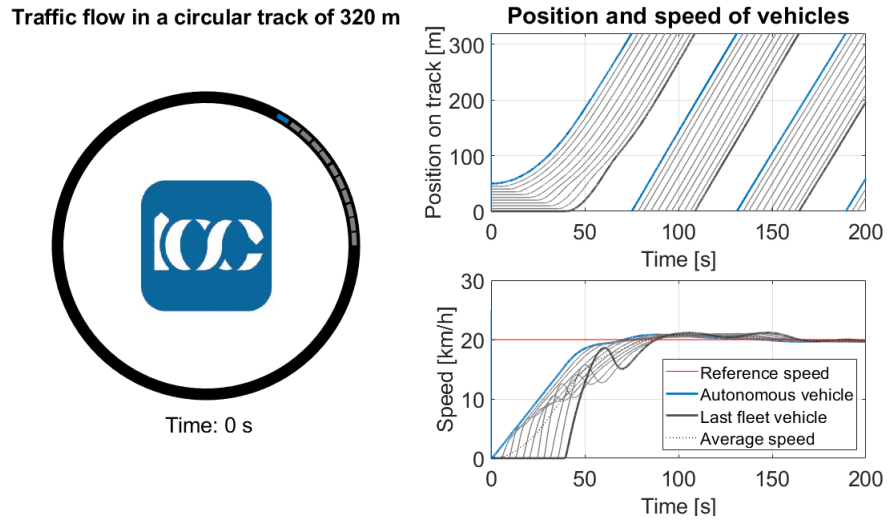

Figure 6.1: Circular track where one controller-equipped autonomous vehicle (blue) is leading one fleet of 10 human driven vehicles governed by IDM.

The results of this simulation are displayed in Figure 6.2 (bottom) along with the same simulation but only replacing the autonomous vehicle by an IDM-governed vehicle (top). With this particular setup and these particular conditions, the IDM-governed vehicles without autonomous vehicle show considerable SG effect. Even though they do not seem to stop completely, they produce important waves, and not even is the

average speed stabilized at a constant value. However, when replacing the leading IDM vehicle by the controller-equipped autonomous vehicle the results are brilliant: the SG effect is completely removed, the average speed is considerably increased and the reference speed is almost perfectly reached.

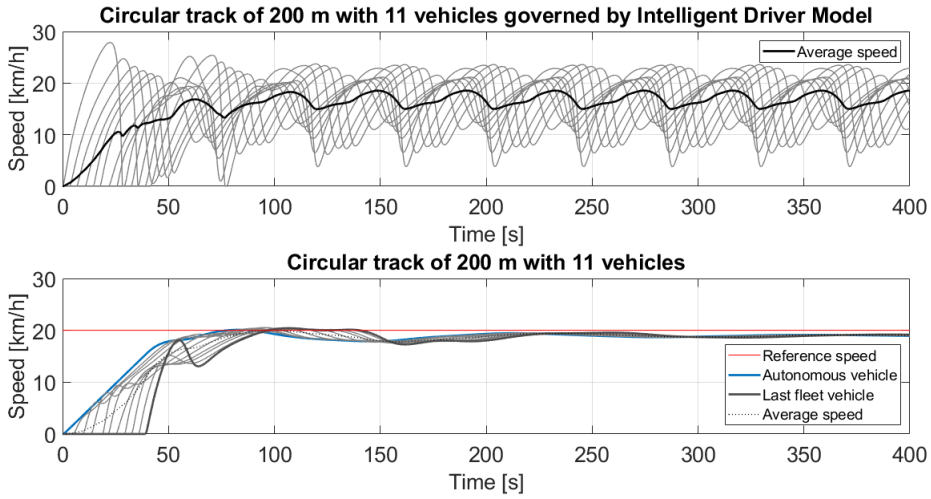

Figure 6.2: Comparison between the behaviour of 11 vehicles governed by IDM (top) and the behaviour of 10 vehicles governed by IDM with 1 autonomous vehicle ahead (bottom).

The results are promising and everything indicates that it is time to try and add another autonomous vehicle and another fleet of IDM-governed human driven vehicles.

6.3 Incorporation of two controller-equipped autonomous vehicles among two fleets of human driven vehicles

This is the final test setup, and it consists of two controller-equipped autonomous vehicles, each leading a fleet of 10 human driven vehicles (see Figure 6.3). So that is a total of 22 vehicles, all of them traveling counterclockwise.

Finally, this is one realistic ensemble because vehicle-to-vehicle communication applies, so now it is possible for the autonomous vehicle #1 to collect data from the human driven vehicle #11, thanks to the autonomous vehicle #12, which is just behind; and the same happens with the data sent to the autonomous vehicle #12 from the human driven vehicle #22 via the autonomous vehicle #1.

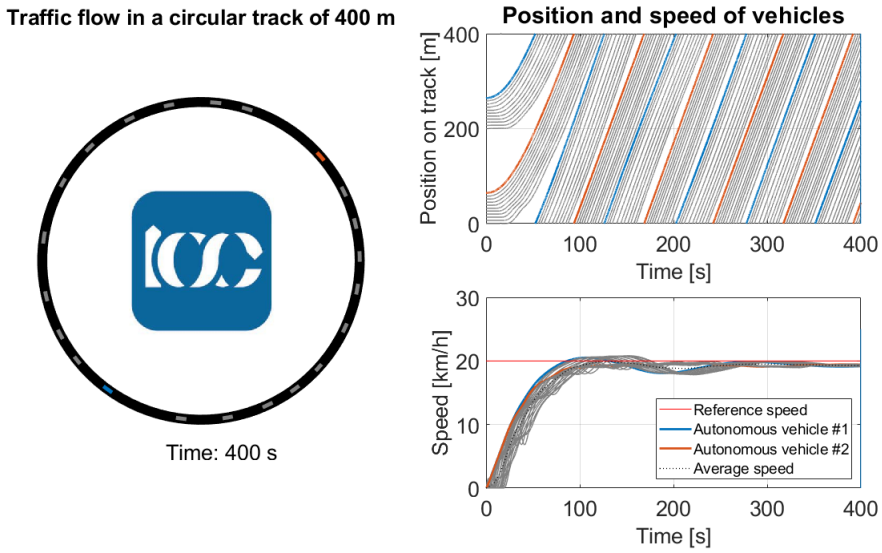

Figure 6.3: Circular track where two controlled autonomous vehicles (blue and orange) are embedded among two fleets of 10 human driven vehicles governed by IDM.

The results of this simulation are displayed in Figure 6.4 (bottom) along with the same simulation replacing both autonomous vehicles by IDM-governed vehicles (top).

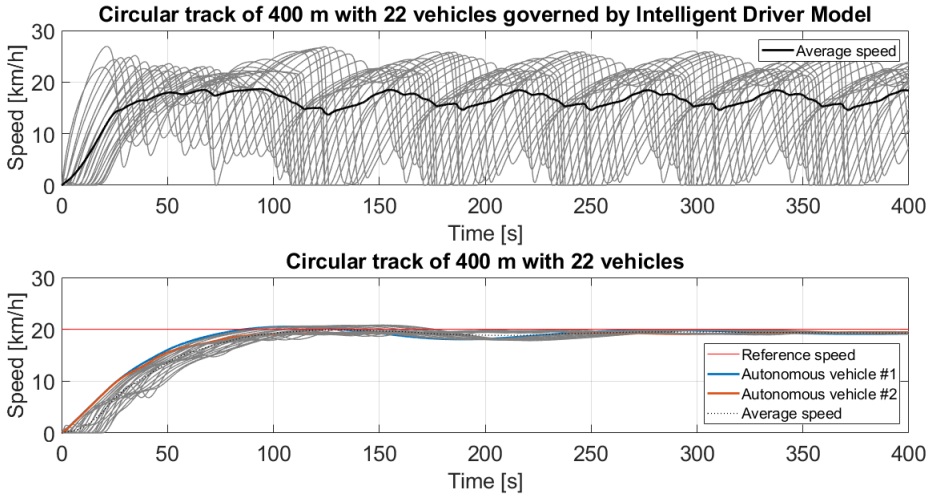

Figure 6.4: Circular track where two controlled autonomous vehicles (blue and orange) are embedded among two fleets of 10 human driven vehicles governed by IDM.

With this setup and these conditions, the IDM-governed vehicles without any autonomous vehicle show even more considerable SG effect, since they even show full stops. The average speed is, again, not stabilized at a constant value. However, when replacing the IDM vehicles #1 and #12 both by a controller-equipped autonomous vehicle the ultimate results are brilliant: the SG effect is completely removed, the average speed is considerably increased and the reference speed is almost perfectly reached.

Conclusions

The comparison between human driving models, MITSIM and IDM resulted in the clear conclusion that the IDM is better imitator of the actual human driving behaviour, or at least the behaviour that this project tries to improve.

A model for a unified fleet of human driven vehicles, treating n vehicles as a unit vehicle with variable length, can be successfully implemented. Some readjustments need to be made regarding delay and variation of length, but the model as a first approach is not a bad deal. In order to deal with the problem of delays, one can explore other control techniques such as frequency methods, or use a Padé approximation for the delay.

A well designed state feedback control with integral action can be good most of the times, but in the case of neglecting the delay of the individual vehicles with respect to the unified fleet is a bad deal.

A simple proportional controller with output feedback can be surprisingly useful and achieve improvement of traffic flow and reduction of Stop and Go effect.

In general, control-equipped autonomous vehicles have been shown to improve human traffic flow; both in terms of average speed and in terms of reduction of Stop and Go effect. Communication between autonomous vehicles is crucial for that purpose.

Bibliography

[1] S. ichi Tadaki et al., *Phase transition in traffic jam experiment on a circuit*. New J. Phys. 15 103034, 2013.

[2] E. Benedito, A. Dòria-Cerezo, C. Kunusch, and J. M. Olm, *Traffic flow-oriented design and analysis of an adaptive cruise control system*. IEEE, 2018.

[3] J. J. Olstam and A. Tapani, *Comparison of Car-following models*. Swedish National Road and Transport Research Institute, 2004.

[4] K. J. Aström and R. M. Murray, *Feedback Systems*. Princeton University Press, 2012.

[5] G. L. Plett, "State-feedback control." `http://mocha-java.uccs.edu/ECE5520/ECE5520-CH06.pdf`, Jun 2019. Accessed on 2019-06-25.

List of Acronyms and Variables

CF	Car Following regime
EB	Emergency Braking regime
FD	Free Driving regime
IDM	Intelligent Driver Model
MITSIM or MTS	Microscopic Traffic Simulator Model
R0	IDM's Regime 0
R1	IDM's Regime 1
SG	Stop and Go effect
UFHDV	Unified Fleet of Human Driven Vehicles
A	Matrix of the dynamics of a linear system
$_A$	Subscript for autonomous vehicles
a	Acceleration of a vehicle or fleet of vehicles
a^{max}	IDM parameter - Maximum acceleration
B	Matrix of the dynamics of a linear system
b^{max}	IDM parameter - Maximum deceleration
C	Matrix of the output of a linear system
D	Scalar of the output of a linear system
d	Length of the circular track
F	Function of a human or autonomous acceleration demand
G	Transfer function of a linear system
$_H$	Subscript for a fleet of human driven vehicles
h	Net bumper-to-bumper distance between vehicles
h^0	IDM parameter - Minimum net bumper-to-bumper distance
$_i$	Subscript
$_j$	Subscript
j	Imaginary unit

K	Matrix of gains of a state feedback system
k	Gain
L	Length of a vehicle or fleet of vehicles
l	Length of a vehicle which is part of a fleet of vehicles
M_p	Maximum overshoot
N	Number of vehicles and/or fleets of vehicles
n	Number of vehicles which are part of a fleet of vehicles
P_d	Desired characteristic polynomial
p	Coefficients of a polynomial
q	Absolute position of a vehicle
R	Radius of a circular track
s	Laplace transform's complex frequency
T	IDM parameter - Safety time headway
T_r	Rise time
T_s	ϵ-settling time
t	Time
u	Control action
v	Speed of a vehicle or fleet of vehicles
v^0	IDM parameter - Desired speed
v_r	Reference speed for control
W_C	Controllability or Kalman matrix
x	State variables of a system
y	Output of a system
z	Integral action for control
z	Zero (root on the numerator of a transfer function)
α	MITSIM parameter - Proportionality factor
β	MITSIM parameter - Speed exponent
γ	MITSIM parameter - Distance exponent
δ	IDM parameter - Acceleration exponent
ζ	Damping coefficient of a second order system
η	Parameter of a fleet of vehicles
θ	Angular absolute position of a vehicle or fleet of vehicles
λ	Pole/eigenvalue

σ	Real part of a pole/eigenvalue
τ	Time constant
ψ	Auxiliary expression regarding a second order system
ω	Angular speed of a vehicle or fleet of vehicles
ω_0	Natural frequency of a second order system
ω_d	Imaginary part of a pole/eigenvalue

List of Figures

List of Tables